Spatiotemporal Variations of Summer Rainfall over Eastern China during 1880–1999①

Li Xiaodong (李晓东), Zhu Yafen (朱亚芬), and Qian Weihong (钱维宏)

Department of Atmospheric Sciences, School of Physics, Peking University, Beijing 100871

(Received January 5, 2002; revised July 15, 2002)

ABSTRACT

By applying rotated complex empirical orthogonal function (RCEOF) analysis on 1880–1999 summer rainfall at 28 selected stations over the east part of China, the spatio-temporal variations of China summer rainfall are investigated. Six divisions are identified, showing strong temporal variability, the middle and lower reaches of the Yangtze River, the Huaihe River, Southeast China, North China, Southwest China, and Northeast China. The locations of all divisions except Southwest China are in a good agreement with those of the rainband which moves northward from Southeast China to Northeast China from June–August. The phase relationship revealed by the RCEOF analysis suggests that rainfall anomalies in the middle and lower reaches of the Yangtze River, Southeast China, and Northeast China are all characterized by a stationary wave, while a traveling wave is more pronounced in the Huaihe River division, North China, and Southwest China. The fourth RCEOF mode indicates that rainfall anomalies can propagate from south of Northeast China across lower reaches of the Huanghe River and the Huaihe River to the lower reaches of the Yangtze River. A 20–25-year oscillation is found at the middle and lower reaches of the Yangtze River, the Huaihe River valley, North China, and Northeast China. The middle and lower reaches of the Yangtze River and Northeast China also show an approximately-60-year oscillation. Northeast China and the Huaihe River division are dominated by a 36-year and a 70–80-year oscillation, respectively. An 11-year oscillation is also evident in North China, with a periodicity similar to sunspot activity. The interdecadal variability in the middle and lower reaches of the Yangtze River, the Huaihe River valley, and North China shows a significant positive correlation with the solar activity.

Key words: empirical orthogonal function (EOF), rotated complex EOF (RCEOF), China summer rainfall, drought and flood anomaly, stationary wave, traveling wave, interdecadal variability

1. Introduction

Recently, global climate change has become a tremendous public concern. Each year, drought and flood hazards directly cause huge loss of life and economic damage. Therefore, better weather prediction is urgently needed. Yet droughts and floods tend to have significant spatial and temporal variability which hinders the investigation. Most previous studies on China rainfall variability were focused on eastern China during the last 50 years (Deng et al. 1989; Chen and Wu 1994; Nitta and Hu 1996; Wang and Wu 1997). Due to the lack of long-term observations, the rainfall anomaly pattern over a longer period (~ 100 years) is poorly understood (Wei et al. 1995). Lately, Wang et al. (2000) reconstructed seasonal and annual rainfall at 35 stations located east of 100°E in China during the period 1880–1998 using both operational rainfall observations as well as historical documents. These 35 stations were evenly distributed over eastern China and thus can provide a good representation of the cov-

①E-mail: zhuyf@pku.edu.cn

ered area. Using both rainfall and temperature variables from this data set, Qian and Zhu (2001) showed that 20–year and 70–year oscillations are pronounced at various stations. But they did not categorize the spatial patterns.

Thus, the motivation of this work is to investigate the spatial and temporal characteristics of China summer rainfall using 1880–1999 rainfall data. To fulfill the task, rotated complex EOF (RCEOF) analysis (Li 1999; Li and Hou 1999) is applied. Wavelet analysis is also used to reveal the periodicity of rainfall at each division.

The paper is organized as follows. Section 2 introduces the data and method of RCEOF analysis. Six flood / drought divisions are defined in section 3.1. The temporal evolution at four selected divisions is described in section 3.2. Sections 3.3 and 3.4 further discuss the interdecadal variability and its relationship to solar activity. The results are summarized in section 4.

2. Data and method

2.1 *Data*

Details of the dataset are provided in Wang et al. (2000). Our interest is focused on the Yangtze River valley and its northern area. Correspondingly, 28 stations are chosen which are located north of 25°N. The distribution of the stations is displayed in Fig. 1. The study period is from 1880 to 1999.

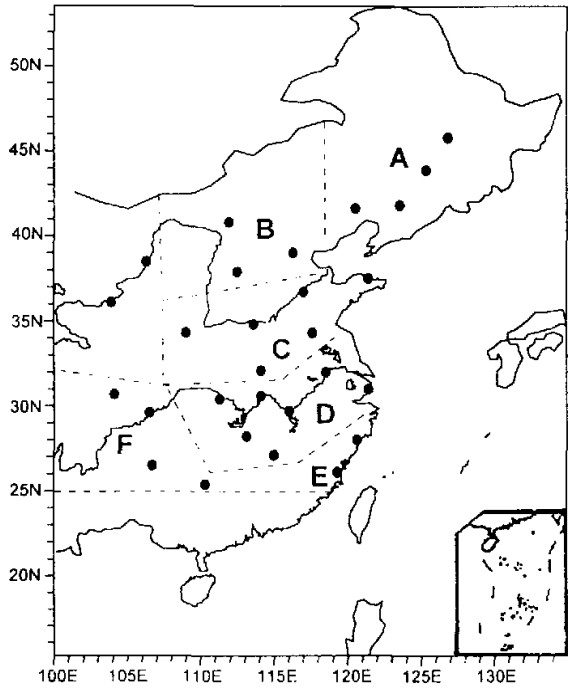

Fig. 1. The location of 28 selected stations marked by dots. The letters (A–F) indicate the six active centers of the RCEOF modes.

2.2 *Origin of the RCEOF method*

Empirical orthogonal function (EOF) analysis was first proposed by Pearson (1902). Since being introduced to the atmospheric sciences by Obukhov (1947), Lorenz (1956), and Kutzbach (1967), EOF analysis has been widely employed in the earth sciences including meteorology, climatology, geology, and oceanography. Its application is greatly facilitated by the improvement of computer technology. Hardy and Hacker (1978) expanded EOF to complex EOF (hereafter CEOF). The traditional idea of CEOF decomposition was introduced to meteorology by Rasmussan and Carpenter (1982). Thereafter, it was improved by Barnett (1983; 1985). The CEOF method has the advantages of both conventional EOF analysis and cross-spectral analysis, which has become a widely used diagnostic tool to detect propagating phase-relations in the geophysical fields (see Barnett 1983, 1985; Horel 1984; and Treberth et al. 1984, for example). In seeking more accurate characteristic patterns, or the " physical" modes, the rotated EOF (hereafter REOF) approach was developed by Richman (1986). REOF supplies a new set of modes by rotating the vector space of the initial EOFs, and improves the physical interpretation of the original field. It has been widely used in meteorological and climatic studies since the 1980s (see Richman 1981; Richman 1986; O'lenic and Livezev 1988; Kelly et al. 1999; and Tu et al. 2000, for example). Based on the methods of EOF, CEOF, and REOF, Li (1999) designed the RCEOF method, which inherits the advantages of the previous methods and avoids their limitations. Details of RCEOF are described in Li (1999) and Li and Hou (1999). This paper focuses on the application of RCEOF in investigating the dry-flood variations in eastern China over the last 120 years.

3. Results

3.1 *Spatial pattern of summer rainfall anomaly*

Figure 2 displays the spatial magnitudes of the first 6 RCEOF modes, which explain 69.4% of the total variance. The value in the upper left corner of each panel in Fig. 2 indicates the percentage of the total variance that the un-rotated mode explains, and the one in the lower left corner is for the rotated mode. The first mode (RCEOF1) accounts for 17.4% of the total variance, while the un-rotated one accounts for 15.5%. The variability center is located at the middle and lower reaches of the Yangtze River (108°–120°E, 25°–33°N), where the summer rainfall anomaly is mainly associated with Meiyu frontal rainfall and the strength of the East Asian summer monsoon (Lau 1992). The percentage that RCEOF2 (Fig. 2b) explains increases from 9.8% to 13.7% after being rotated. The high variability center is in the Huaihe River valley, a transition zone in the mid-latitude where summer rainfall is influenced by the onset and retreat of the East Asian summer monsoon and the location of the Meiyu front. Mode RCEOF3 (Fig. 2c) accounts for 12.9% of the total variance, compared with 8.2% for the un-rotated mode. The variability center is located south of the Yangtze River. Mode RCEOF4 accounts for 9.6% of the total variance compared with 23.2% before rotation. It has three variability centers located in the lower reaches of the Yangtze River, Sichuan basin and North China (Fig. 2d). Mode RCEOF5 (Fig. 2e) accounts for 9.0% of the total variance compared with 6.7% before rotation. The variability centers are located on the west of the Hunan Province and on the east of the Yunnan Guizhou Plateau. Mode RCEOF6 explains 6.8% of the total variance compared with 6.0% before rotation. The variability center is located in Northeast China and in the middle reaches of the Yangtze River.

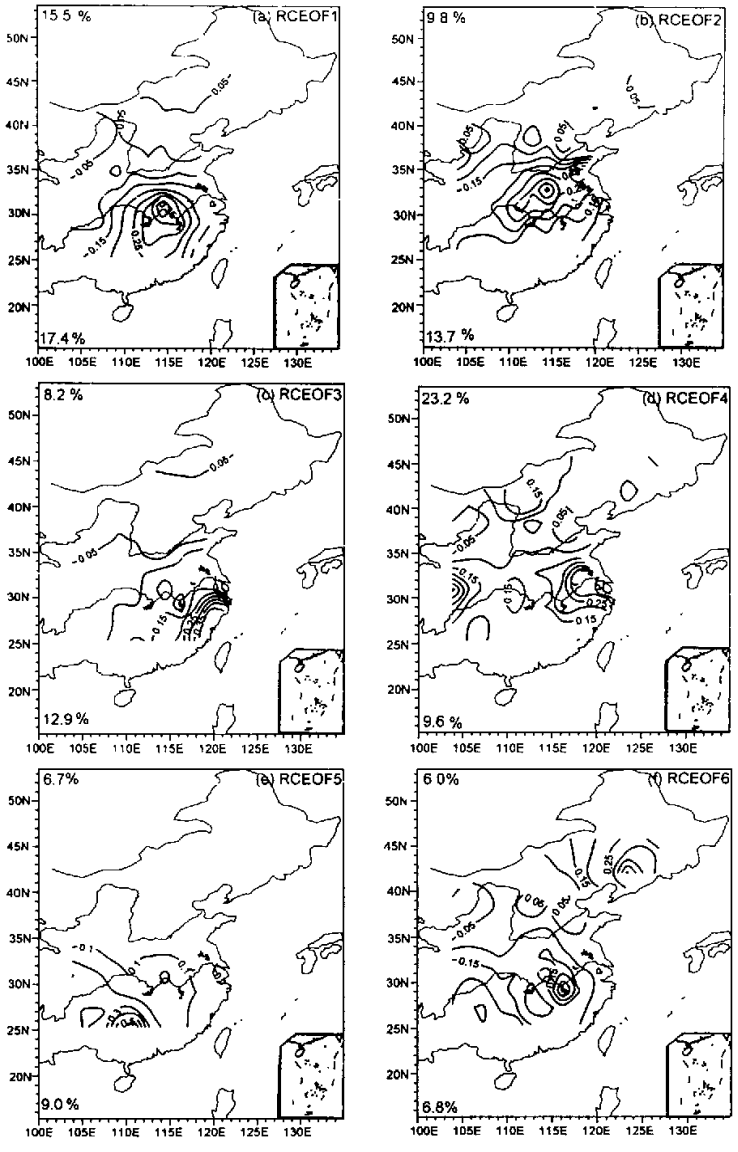

Fig. 2. Amplitude of the leading 6 RCEOF mode spatial patterns of eastern China summer rainfall. The value in the upper left corner of each panel indicates the percentage of the total variance that the un-rotated mode explains, while the one in the lower left corner represents the rotated mode.

Using rotated principle component analysis (RPC), summer rainfall variability in recent several decades has been analyzed by Huang (1991) and Wang and Wu (1997). Huang (1991) found that the first mode features anomalies at the middle and lower reaches of the Yangtze River having an opposite sign compared with the rest of China. In the first mode that Wang

and Wu (1997) found, the Yangtze River and the Huaihe River valleys have an opposite sign compared with the Hetau area and South China. These two patterns resemble our first and second modes. Both RPC and RCEOF are efficient tools for analyzing spatial variability, except that RCEOF is more effective in revealing wave patterns. Using 160–station summer rainfall data for China in the period of 1951–1994, the first two EOF modes found by Nitta and Hu (1996) are also similar with our results. Liao and Zhao (1992) summarized three China summer rainband patterns using June–August rainfall anomaly since 1951. Our first and third modes resemble their pattern II. Our second and fourth modes resemble their patterns III and I, respectively. Therefore, the RCEOF analysis based on 120–year summer rainfall data at 28 stations in China can produce reasonable variability patterns. Such a long–term record can also provide valuable information on China's regional climate change and its possible connections with external forcings such as solar activity, volcano eruptions, and the greenhouse effect.

Located in the Asian summer monsoon domain, China's rainfall has a strong seasonality. The summer rainband movement and large–scale rainfall are both significantly influenced by the summer monsoon. All the above six patterns except the 5th mode are linked by the rainband marching northward from June to August. The rainband jumps to the Yangtze River valley from Southeast China in mid–June, which marks the onset of Meiyu. It stretches from the Sichuan basin northeastward to south of Japan. It is most pronounced in the middle and lower reaches of the Yangtze River. The rainfall can usually last for 20 days. Our first RCEOF mode is associated with Meiyu rainfall. When Meiyu ends in mid–July, the rainband jumps northward again across Huanghe River and the Huaihe River. It arrives in the Hetao area, North China, and Northeast China at the end of July. In mid–August, the rainband reaches its northern border and stays there till late–August. The second RCEOF mode reflects the rainband's motion across Huanghe River and the Huaihe River. The 4th and 6th modes reflect the North and Northeast China summer flood and drought. By the end of August, the rainband quickly retreats southward. It arrives in the Yangtze River valley in about half a month and disappears.

Figure 3 displays the phase of the six RCEOF modes. While the length of the vector indicates the strength of the variability, propagation can be reflected by the spatial phase vectors. The variability centers in Fig. 3 are generally in agreement with those in Fig. 2, except that Fig. 3 shows that the six modes have different wave characteristics. The large vectors of the first mode (Fig. 3a) all favor the same direction, which implies that the first mode is a stationary wave. Figure 3b shows that there is a wave propagating eastward in the middle and lower reaches of the Huaihe River, and stationary wave characteristics dominate in the upper Huaihe River valley and the middle and lower reaches of the Huanghe River surrounding area. A stationary wave is also evident in Southeast China in Fig. 3c. Figure 3d shows that there are two active centers with one in North China and the other in the lower reaches of the Yangtze River. These two areas have opposite phase, which suggests a flood (drought) in North China is associated with a drought (flood) in Southeast China. The direction of the vectors suggests that a stationary wave dominates in North China and a propagating wave dominates in the middle and lower reaches of the Yangtze River.

Spatial phase vectors indicate that the anomaly first appears to the south of Northeast China. It propagates anticlockwise across the east part of Hebei Province, the lower reaches of the Huanghe River and the Huaihe River, and intensifies in the lower reaches of the Yangtze River. The southward propagation feature is quite evident. In the fifth mode (Fig. 3e),

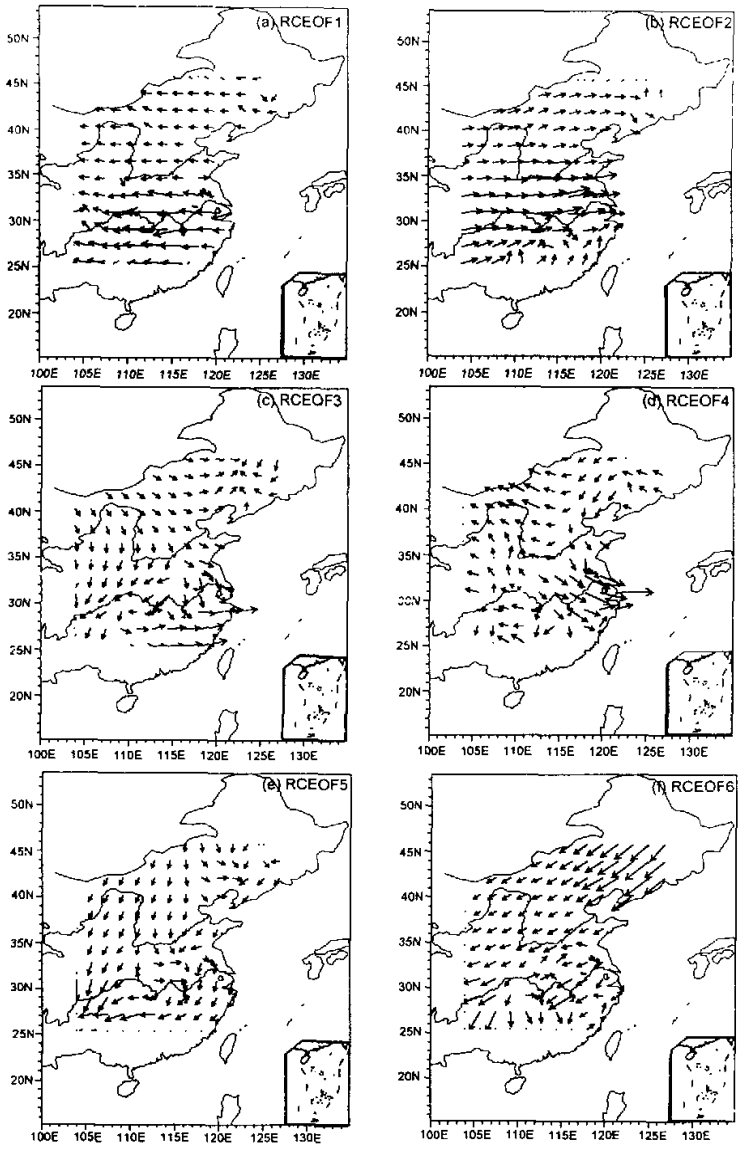

Fig. 3. Spatial phase vectors of the leading 6 RCEOF mode.

the strong variability in Southwest China results from the interaction of two propagating waves: a westward propagating wave and a northeastward propagating wave. The consistent direction of the vectors of the sixth mode (Fig. 3f) in Northeast China suggests a stationary wave causes the rainfall anomaly there. The direction is also similar with those in the middle reaches of the Yangtze River, which implies that rainfall anomalies in these two areas have the same phase. For example, a flood prevailed in both areas in the summer 1998.

Defined by the contours of the six RCEOF modes enclosing values larger than 0.15, six active centers are identified: (A) Northeast China, (B) North China, (C) the Huaihe River valley, (D) the middle and lower reaches of the Yangtze River, (E) Southeast China, and (F) Southwest China (refer to Fig.1). Some adjacent divisions have a small overlapping area. Thus, RCEOF analysis provides a subjective method to categorize drought / flood divisions, which will facilitate regional climate study. Although there are only 2–6 stations in each division, we have confirmed through statistical test that each station can well represent the whole division. For example, Fig. 4 gives the correlation map between the North China division (containing 3 stations) and 160 stations nationwide in summer from 1951 to 1999. The thick solid line indicates the 0.05 significance level (0.281 contour). It is found that most areas in North China can pass the 95% confidence level. Therefore, the three selected stations provide a good representation of the whole division. Because the Yangtze River valley and its northern area have observed frequent drought (flood) disasters, temporal variability in the related divisions is discussed in the following section.

3.2 *Temporal variability of regional rainfall in the last* 120 *years*

In order to investigate the temporal evolution of drought / flood in the selected divisions, the 1880–1999 average of all stations in a division is calculated separately for each division. The anomalies in divisions A, B, C, and D are displayed in Fig. 5, where the thin solid line is the rainfall anomaly and the smoothed thick line indicates a 10th-order polynomial fitting. According to the thick line, 3–4 cycles are found in each division during the whole period. In division A, drought dominates in the 1900s–1910s and the 1970s to the late 1980s, while flooding prevails in the 1880s–1890s, from the late 1940s to 1960s, and the late 1980s to the late 1990s. The anomalies are relatively small during the 1920s to the 1940s. Currently, the

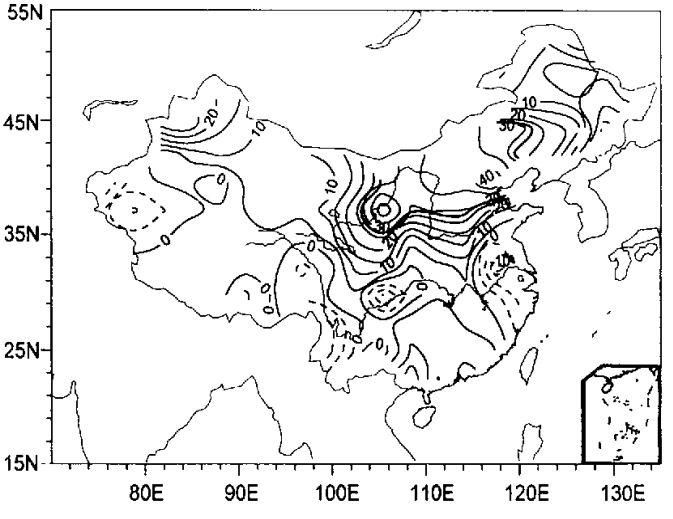

Fig. 4. Correlation coefficient of 1951–1999 summer rainfall between the average of the three selected stations in North China and the 160 stations nationwide. The thick line denotes the 95% confidence level.

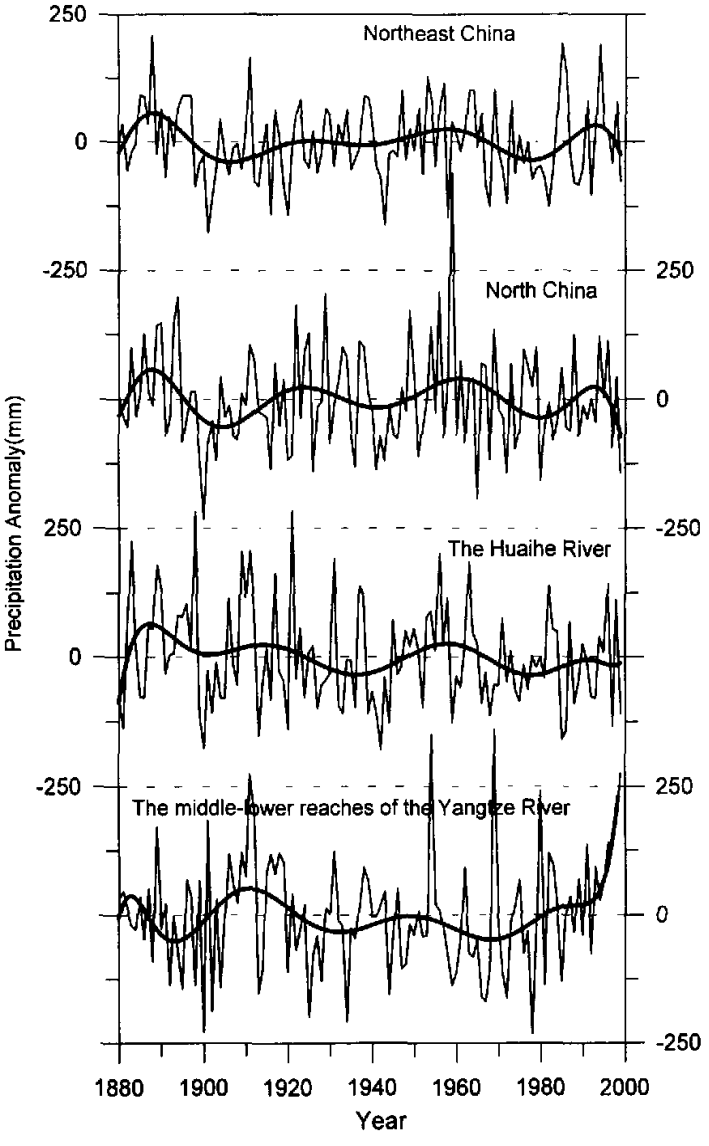

Fig. 5. Time series of averaged rainfall anomalies for divisions A–D (thin solid line) and a 10th-order polynomial fitting (smooth thick line).

trend is towards drought. In division B, dry periods are the mid–1890s to the late 1910s, the 1930s–1940s and the 1970s–1980s. Four wet periods are found: the 1880s to mid 1890s, the late 1910s to 1920s, the 1950s–1960s and the late 1980s to the 1990s. The last wet period is the shortest one, where its termination quickly leads to the start of another dry period in the late 1990s. In division C, there are two major wet periods: from the 1880s to the mid–1920s and

the 1950s–1960s and two significant dry periods: the mid–1920s to the 1940s and the 1970s–1999. In division D, the wet periods are from the 1900s to the mid–1910s and the 1980s–1999, while the dry periods are the mid–1880s–1890s and 1920s–1970s. By the summer of 1999, the increasing trend is still pronounced.

3.3 *Interdecadal variability*

In order to investigate the interdecadal variability in China summer rainfall in the last 120 years, wavelet analysis is carried out in each division. The wavelet transfers of the time coefficients of the RCEOF in divisions A–D are displayed in Fig. 6. It is found that division D is dominated by 15–year, 25–year, and 60–year oscillations (Fig. 6d1). The 15–year oscillation is significant before 1990. It becomes stronger after the 1930s. As for the 25–year oscillation, it seems to intensify around 1900. The 60–year oscillation is evident throughout the whole period. A 25–year and a 70–80–year oscillation are found for division C (Fig. 6c1). A 15–year oscillation is also clear in late 20th century. A 10–year, a 20–year and a 60–year oscillation coexist in division B. The 20–year oscillation becomes significant after the 1920s and intensifies in the latter half of the century. Both the 10–year oscillation and the 60–year oscillation are clear for the whole period, except the 60–year oscillation is relatively weak. A 20–year oscillation and a 30–36–year oscillation are found in division A. The 20–year oscillation becomes relatively strong after the 1930s and the 30–36–year oscillation is more persistent.

The right–hand panels of Fig. 6 display the variance of the wavelet coefficients transferred from RCEOF time coefficients in divisions A–D. A 2–year oscillation and a 6–year oscillation are pronounced at all four divisions. Since the interdecadal variability is of most interest here, only the associated periodicities are listed in Table 1.

Table 1. Dominant interdecadal time scales at Division A–D

Division	Period (years)		
A		20	36
B	11	22	about 60
C	15	25	70–80
D	15	25	about 60

In summary, it is found that (a) the summer rainfall in the recent 120 years has a 20–25 year oscillation in each division (A–D); a 60–year oscillation also exists in divisions D and B; a 15–year oscillation is found in divisions D and C; division A is dominated by a 36–year oscillation; a 70–80–year oscillation is pronounced in division C; an 11–year oscillation is found in division B, which is the same as the periodicity of sunspot activity, and (b) division B is in a negative phase in the late 1990s with regard to both the 60–year oscillation and the 20–year oscillation.

3.4 *Interdecadal oscillation and the solar activity*

Solar radiation, volcano eruption, and human activity are usually considered as the major factors that caused the change in the climate during the last century (Wang 1994). Among them, the sun is the only persistent external forcing on the earth. The following will discuss how the sun's activity affects China's regional climate, especially on the interdecadal time scale.

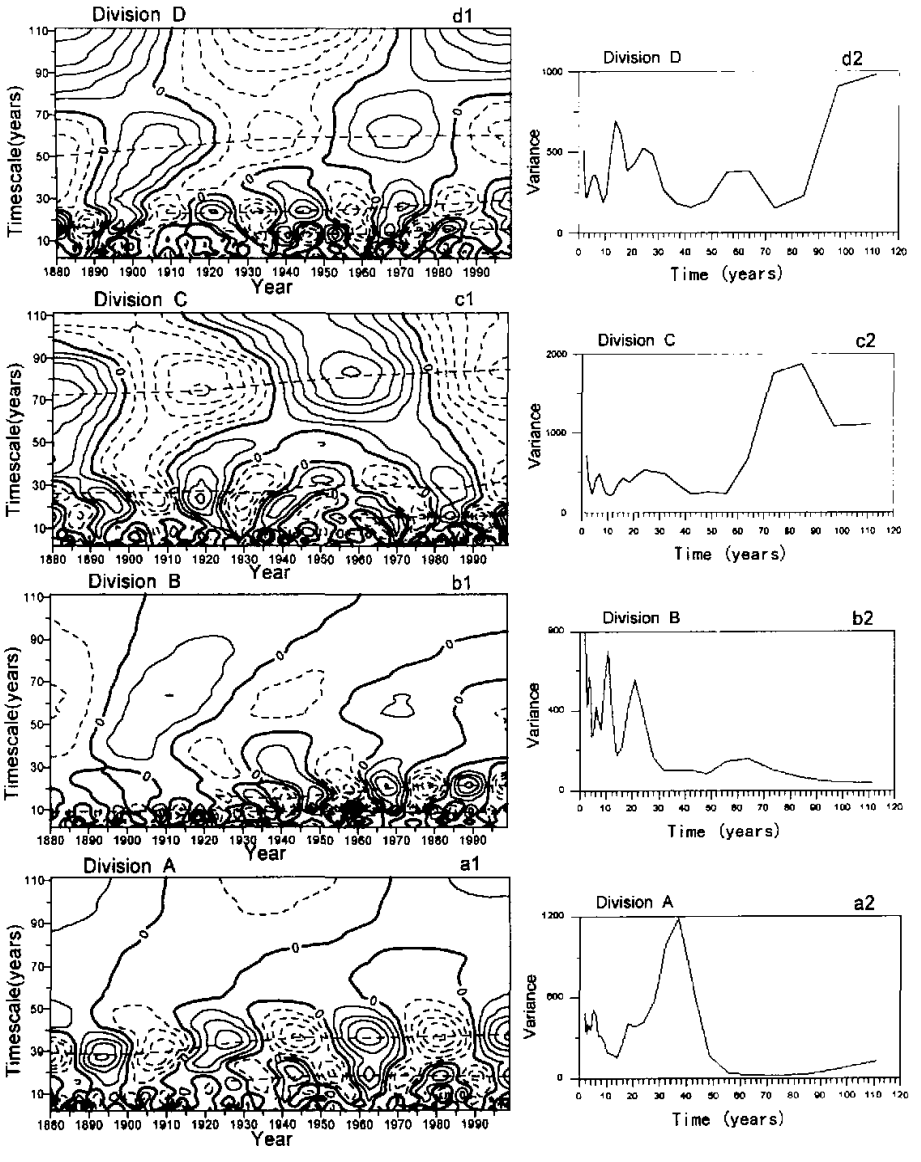

Fig. 6. Wavelet transfer of RCEOF time coefficients at division D (d1), C(c1), B(b1), and A(a1), and corresponding variance of wavelet coefficients (d2, c2, b2, and a2).

Figure 7 displays the time series of the solar radiation coefficient and its wavelet transfer. The solar radiation coefficient for the period 1894–1993 is adopted from North and Stevens (1998). Its wavelet transfer shows that the solar activity is dominated by 11–year and 40–year oscillations. The 11–year oscillation is more pronounced throughout the whole period. In

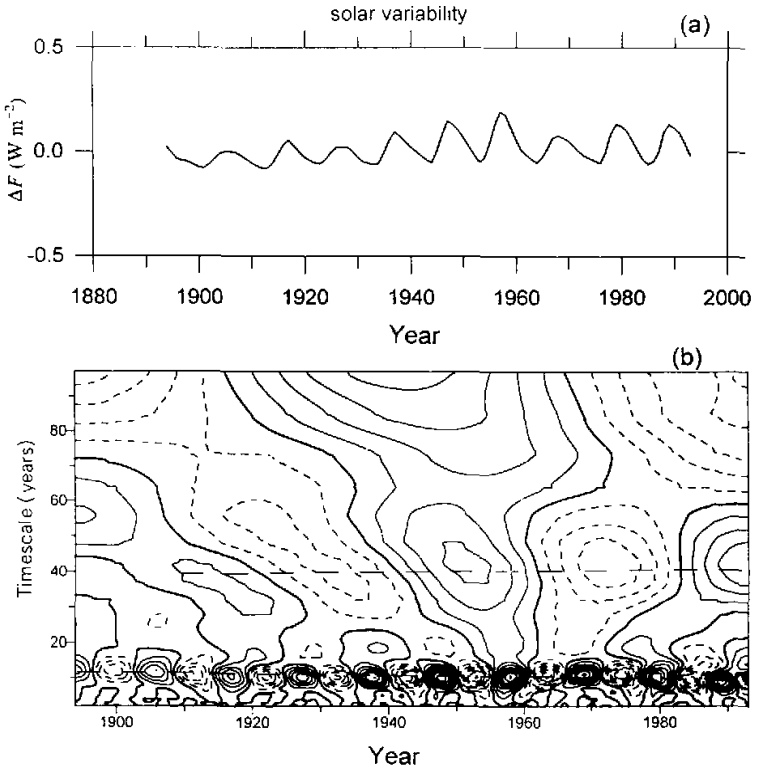

Fig. 7. Time series of the solar radiation coefficient (a) and its wavelet transfer (b). Note the prominent oscillation at 11 years and at 40 years.

order to investigate its possible influence on China's regional climate, the linear correlations between the solar radiation coefficient and RCEOF time coefficients in divisions A–D are calculated. They are −0.076, 0.281, 0.092, and −0.027 for divisions A, B, C, and D, respectively. The correlation coefficient for division B exceeds the 95% confidence level, which suggests that the summer rainfall anomaly in North China may be related to the anomalous solar activity. The correlations in the other three divisions are all insignificant.

In order to focus on the interdecadal time scale, we summed the wavelet transfer components with period $\geqslant$ 8 years using both the solar radiation components and the RCEOF time coefficients for divisions A–D, and reconstructed a new time series which contains only interdecadal variability. Correlations are recalculated between the filtered solar radiation coefficient and the filtered time series in divisions A–D. They are −0.048, 0.223, 0.357, and −0.291 for divisions A, B, C, and D, respectively. The correlation coefficients for divisions D, C, and B exceed the confidence levels of 99%, 99.9%, and 95%, respectively. This suggests that these three divisions are closely influenced by the solar activity on the interdecadal time scale, with division A being the exception.

4. Summary

The spatial and temporal evolution of summer rainfall over the eastern part of China is investigated by RCEOF analysis using rainfall data of 28 stations during the period 1880–1999. The results are as follows.

(1) Six divisions are identifed, namely Northeast China, North China, the Huaihe River valley, the middle and lower reaches of the Yangtze River, Southeast China, and Southwest China. Except for Southwest China, all the divisions reflect the northward movement of the summer rainband from June to August. The phase relationship suggests that flood / drought in the middle and lower reaches of the Yangtze River, Southeast China, and Northeast China is mainly associated with a stationary wave, while that in the Huaihe River division, in North China, and in Southwest China is mainly associated with propagating waves. According to the 4th RCEOF mode, rainfall anomalies in the northern and southern parts of China have opposite phase. This pattern can propagate from south of Northeast China across the Huaihe River and the Huanghe River region to the lower reaches of the Yangtze River.

(2) The Huaihe River division has been in the dry phase since the 1970s to the end of the 20th century. After a severe drought from the 1970s to the late 1980s and a relative normal 1988 summer, North China entered a short wet phase. After the wet phase had lasted for 7–8 years, it was replaced by a severe drought. The middle and lower reaches of the Yangtze River entered a wet phase after 1980. Its rainfall anomaly quickly increased in the 1990s, which led to a significant flood, in contrast to the drought in northern China.

(3) A 20–25–year oscillation is found in the summer rainfall in all four divisions of interest (A–D); divisions D and B show a 60–year oscillation; division A is dominated by a 36–year oscillation and division C is dominated by a 70–80–year oscillation; an 11–year oscillation is found in division B, which agrees well with the periodicity of sunspot activity.

(4) The interdecadal variability of summer rainfall in divisions D, C, and B is significantly correlated with solar activity. The correlation coefficients exceed the confidence levels of 99%, 99.9%, and 95%, respectively.

Acknowledgments. The authors wish to thank Professor Wang Shaowu from the Department of Atmospheric Sciences of Peking University, who generously provided the China Summer Rainfall Station Data used in this study. This research was supported by the National Key Program for Developing Basic Sciences in China (G1999043405).

REFERENCES

Barnett, T. P., 1983: Interaction of the monsoon and Pacific trade wind system at interannual time scales, Part 1: The equatorial zone. *Mon. Wea. Rev.*, **111**, 756–773.

Barnett, T. P., 1985: Three-dimensional structure of low frequency pressure variations in the tropical atmosphere. *J. Atmos. Sci.*, **42**, 2798–2803.

Chen L. T., and Wu R. G., 1994: Categorization and characteristics of flood / drought variations in eastern China. *Scientia Atmospherica Sinica*, **18**(5), 586–595 (in Chinese).

Deng A. J., Tao S. Y., and Chen L. T., 1989: EOF analysis of China summer rainfall. *Scientia Atmospherica Sinica*, **13**(3), 289–295 (in Chinese).

Hardy, D. M., and J. M. Hacker, 1978: On the vertical transports in the northern atmosphere. Part II: Vertical eddy momentum transport for summer and winter. *J. Geophys. Res.*, **83**, 1305–1318.

Horel, J. D., 1984: Complex principal component analysis: Theory and examples. *J. Climate and Appl. Meteor.*, **23**, 1660–1673.

Huang J. Y., 1991: Spatiotemporal characteristics of China summer temperature and precipitation. *Scientia Atmospherica Sinica*, **15**(3), 124–132 (in Chinese).

Kelly, P. M., and P. D. Jones, 1999: Spatial patterns of variability in the global surface air temperature data set. *J. Geophys. Res.*, **104**, 24237–24256.

Kutzbach, J., 1967: Empirical eigenvectors of sea level pressure, surface temperature, and precipitation complex over North America. *J. Appl. Meteor.*, **6**, 791–802.

Li X. D., 1999: Rotated complex empirical orthogonal functions (RCEOF) analysis–Part I: Theory and examples. *Acta Meteor. Sinica*, **13**, 1–10.

Li X. D., and Hou Z. X., 1999 : Rotated Complex Empirical Orthogonal Functions (RCEOF) analysis–Part II: Theory and examples. *Acta Meteor. Sinica*, **13**, 212–225.

Lorenz, E. N., 1956: *Empirical orthogonal functions and statistical weather prediction*. MIT, Dept.of Meteorology, Science Report 1–49.

Lau, K.–M., 1992: The East Asian summer monsoon rainfall variability and climate teleconnections. *J. Meteor. Soc. Japan*, **70**, 211–241.

Liao Q., and Zhao Z., 1992: Mechanisms for seasonal prediction of the distribution of eastern China summer rainfall. *Quart. J. Applied Meteor.*, **3**, (Suppl.), 1–9 (in Chinese).

Minobe, S., 1997: A 50–70 year climatic oscillation over the North Pacific and North America. *Geophys. Res. Lett.*, **24**, 683–686.

Nitta, T., and Z. Z. Hu, 1996: Summer climate variability in China and its association with 500 hPa height and tropical convection. *J. Meteor. Soc. Japan*, **74**, 425–445.

Obukhov, A. M., 1947: Statistically homogeneous fields on a sphere. *Usp. Mat. Navk.*, **2**, 196–198.

O'lenic E. A., and R. E. Livezev, 1988: Practicable considerations in the use of rotated principal component analysis in diagnostic studies of upper–air height fields. *Mon. Wea. Rev.*, **116**, 1682–1689.

Pearson K., 1902: *On lines and plans of closest fit to system of points in space philos. Mag.*, **6**, 559–572.

Qian W. H., and Zhu Y. F., 2001: Climate change in China from 1880 to 1998 and its impact on the environmental condition. *Climatic Change*, **50**, 419–444.

Rasmusson, E. M., and T. H. Carpenter, 1982: Variations in tropical sea surface temperature and surface wind field associated with the Southern Oscillation / El Niño. *Mon. Wea. Rev.*, **110**, 354–384.

Richman, M.B., 1981: Obliquely rotated principal components: An improved meteorological maptyping technique? *J. Appl. Meteor.*, **14**, 1223–1235.

Richman, M. B., 1986: Review article, rotation of principal components. *J. Climatol.*, **6**, 293–355.

Treberth, K. E., and W. T. K. Shin, 1984: Quasi–biennial fluctuations in sea level pressures over the Northern Hemisphere. *Mon. Wea. Rev.*, **112**, 761–777.

Tu Q., Deng Z., and Zhou X., 2000: Regional characteristics of temperature anomaly in China. *Acta Meteor. Sinica*, **58**(3), 288–296 (in Chinese).

Wang S., 1994: *Introduction to Climate System*, China Meteorological Press, Beijing, 250pp (in Chinese).

Wang S., Gong D., Ye J., and Chen Z., 2000: Time series of four–season precipitation in eastern China and its variability. *Acta Meteor. Sinica*, **55**(3), 281–293 (in Chinese).

Wang X., and Wu G., 1997: The anomalous pattern of China summer rainfall and its relationship with the subtropical high pressure system. *Scientia Atmosppherica Sinica*, **21**(2), 161–169 (in Chinese).

Wei F., Zhang X., and Li X. D., 1995: Distribution and interannual variation of drought / flood in eastern China in the last century using CEOF analysis. *Acta Meteor. Sinica*, **6**, 454–460 (in Chinese).

近百年中国东部夏季降水的时空变率

李晓东 朱亚芬 钱维宏

摘 要

利用中国东部 25° N 以北 28 个站 1880—1999 年夏季季降水序列，用旋转复经验正交函数(RCEOF)方法，研究了中国东部地区百年干湿的时空演变规律。结果表明，夏季降水空间变率大值区依次为：长江中下游地区、淮河流域、江南、华北、西南及东北。除西南外的 5 个关键区大体上反映了从 6 月到 8 月夏季雨带自南向北推进所滞留的地区。旋转空间位相分布揭示了长江中下游地区、江南、东北的旱涝异常主要表现为驻波振动特征；而淮河流域、华北、西南地区显示出降水异常信号具有部分的行波特征。尤其第 4 空间模显示出旱涝异常信号从东北南部可沿着黄淮下游传到长江下游地区。对于近百年中国东部地区夏季干湿变化，长江中下游地区、淮河流域、华北及东北四个地区都存在 20–25 年时间尺度的周期振荡；长江中下游地区及华北地区都存在准 60 年时间尺度的振荡周期；东北地区主要表现出 36 年时间尺度的振荡周期；淮河流域存在明显的 70–80 年时间尺度的振荡周期；华北地区存在的 11 年时间尺度的振荡周期恰好与太阳黑子活动的 11 年周期相一致。在年代际时间尺度(包括次年代际时间尺度)上，长江中下游、淮河流域及华北地区的夏季降水的变化与太阳活动有显著的正相关。

关键词：经验正交函数(EOF)，旋转复经验正交函数(RCEOF)，夏季降水，旱涝异常，驻波，行波，年代际，中国东部